JOURNAL OF PHYSICAL ORGANIC CHEMISTRY, VOL. 9, 419–426 (1996)

THEORETICAL STUDY OF THE REACTION OF P^+ WITH METHANE

JESUS R. FLORES

Departamento de Quimica Pura y Aplicada, Area de Quimica Fisica, Facultad de Ciencias, Campus de Orense, Universidad de Vigo, 32004 Orense, Spain

The dynamics of the reaction of P^+ with methane were studied by means of a combination of an approximate classical trajectory method and RRKM theory, using accurate *ab initio* computations of the relevant minima and saddle points of the lowest singlet and triplet potential energy surfaces. The results were compared with those of gas-phase experiments obtained at 300 K. Computed rate coefficients are given for a wide range of temperatures from 40 to 1000 K and may be useful in the modelling of interstellar chemistry, where the reaction of P^+ with methane is believed to play a crucial role in the synthesis of small molecules containing a P—C bond. The results appear to imply that an intersystem crossing process may play a key role in the reaction dynamics.

1. INTRODUCTION

The reaction of P^+ with methane is believed to be the crucial step in the production of simple molecules with P-C bonds in interstellar space.[1,2] Partly for this reason, several gas-phase experimental studies have been carried out,[3,4] in addition to a theoretical study of the lowest lying potential energy surfaces (PES) of the $(PCH_n)^+$ $(n=2,3)$ systems that included a short discussion on the most likely path for this reaction.[5] The experimental results, obtained at 300 K and very low pressures, indicate that the only product is $(PCH_2)^+ + H_2$ and agree on the value of the rate coefficient (k_{bim}) [$9{\cdot}4\times10^{-10}$ (Ref. 3) and $9{\cdot}6\times10^{-10}$ (Ref. 4) cm^3 $molecule^{-1}$ s^{-1}]. However, these studies do not provide any insight into the nature of the product (electronic state, molecular geometry) or into the reaction dynamics or values for the rate coefficient at lower temperatures, which are much needed in the modelling of interstellar space chemistry.[6] The theoretical study[5] concentrated on a search for the saddle point for this process, but the theoretical level employed (unrestricted Hartree–Fock theory[7]), that neglects the so called dynamic and, to some extent, static electron correlation, was not adequate to lead to reliable conclusions.

It should also be pointed out that the reaction of P^+ with methane is interesting on its own merit, in order to understand the dynamics of gas- phase reactions involving small molecules. We have already studied, using a method similar to that employed in this work, the reactions of P^+ with water and Si^+ with ammonia.[8,9] One of the conclusions of these studies was that the experimental values of the rate coefficients corresponding to the whole bimolecular process (k_{bim}), cannot be reproduced without correcting the rate of the capture step (k_c) with a factor f representing the fraction of PES which become nearly degenerate at infinite separation of the reactants and are attractive. In addition, we concluded that the nature of the PES (repulsive or attractive) should be identified by taking into account their height throughout the reaction path, not just at large separations of the reactants.[9] Dateo and Clary[10] suggested that the rate coefficients for reactions of open-shell ions with molecules will normally obey the relation $k_c > k_{bim} > fk_c$, but it is not clear which factors may eventually bring k_{bim} closer to k_c. In this respect, the reaction of P^+ with methane is especially interesting, because it has been found that the experimental rate coefficient (obtained at 300 K) is close to a capture rate computed using a model that includes the charge-induced dipole interaction ($11{\cdot}5\times10^{-10}$ cm^3 s^{-1} $molecule^{-1}$),[4] in contrast to the reaction of P^+ with water for instance.[4,8]

In this work, we employed a method advocated by Phillips[11–13] for computing rate coefficients for gas-phase reactions without activation energy, in the low-pressure limit. It consists of two steps. First, we use an approximate classical trajectory method that can incorporate all relevant contributions to the long-range potential, and chemical interactions through a Morse potential to compute the capture rate and also the energy distribution of the collision complex;[11,13] in this particular case, we take into account charge–induced dipole and

CCC 0894–3230/96/060419–08

Received 29 July 1995
Revised 16 January 1996

charge–quadrupole potentials and a Morse potential determined through *ab initio* computations. In the second step, we employ the energy distribution, in addition to microscopic rate coefficients $[k(E)]$, to compute canonical rate coefficients $[k(T)]$. The microscopic rate coefficients $k(E)$ are obtained by computing the density and sum of states through the Beyer–Swinehart algorithm as implemented by Gilbert.[14] Details of the procedure are given in Refs 11 and 13–16. An appealing feature of this method is that it requires only the computation of the critical points of the PES, namely some local minima and saddle points; this computation, however, must be made accurately, as Gilbert and Smith[15] have strongly emphasized. Nowadays this is possible for small- and medium-sized molecules for instance through the Gaussian–1 (G1) and Gaussian–2 (G2) methods developed by Pople and co-workers.[17,18]

DETAILS OF THE *AB INITIO* COMPUTATIONS

As we stated in the Introduction, we employ the G1 and G2 methods[17,18] for the computation of the important points of the PES, but introducing a few minor modifications. It should be recalled that the G1 and G2 methods are based on the approximate separability of several contributions to the electronic energy that can be written as corrections to the energy of a basic level of computation. Geometries have been optimized at several levels of computation, but we have normally made use of those computed at the MP2(full)/6–31G* level (second-order Møller–Plesset[19] theory with the 6–31G* basis set,[20] including all electrons in the correlation computation) in order to carry out the computation of the electronic energy with correlated methods. However, some minima and saddle points have been located with other methods such as multiconfiguration Hartree–Fock (MCSCF) within the complete active space formulation (CASSCF) [21], and quadratic configuration interaction,[22] which we consider more reliable where there are significant static correlation effects. We have normally employed the vibrational frequencies determined at the MP2(full)/6–31G* level

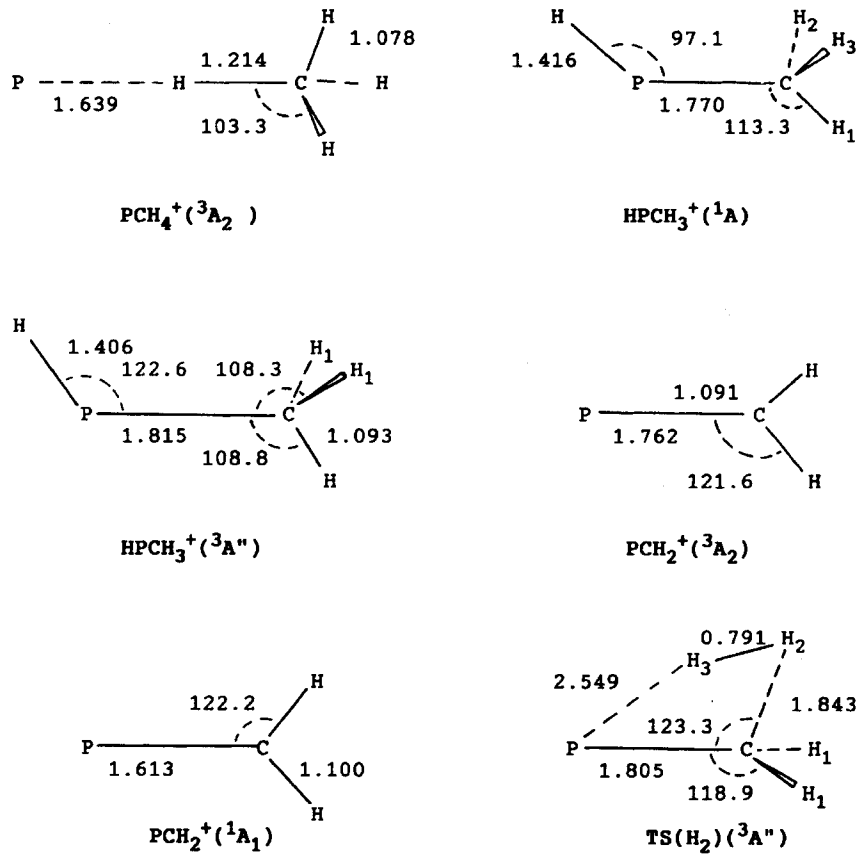

Figure 1. *Continued*

using analytical gradient techniques. For open-shell species we have computed the $\Delta E(+)$, $\Delta E(2df)$ and Δ corrections using spin-projected Møller–Plesset (MP) values[23] instead the unprojected values in the original G1 and G2 theories.[17,18] The computations were made with the Gaussian-90 program package,[24] except for the MCSCF computations, which were carried out with the GAMESS program.[25]

RESULTS AND DISCUSSION

We do not intend here to provide very detailed information about the lowest PES of the $(PCH_4)^+$ system; we only made accurate computations on the minima and saddle points which are likely to be involved the the dynamics of the reaction of P+ with water. In any case, all details of our computations are available upon request.

There are two relevant minima in the lowest triplet PES. $PCH_4^+(^3A_2)$ can be considered basically as ion–molecule complex formed by P^+ and methane; however, there is an incipient but relatively strong P—H bond (see Figure 1). It must be pointed out that the molecular geometry shown in Figure 1 for this system was obtained at the MCSCF/6–31G** level, using a complete active space formulation[21] with six

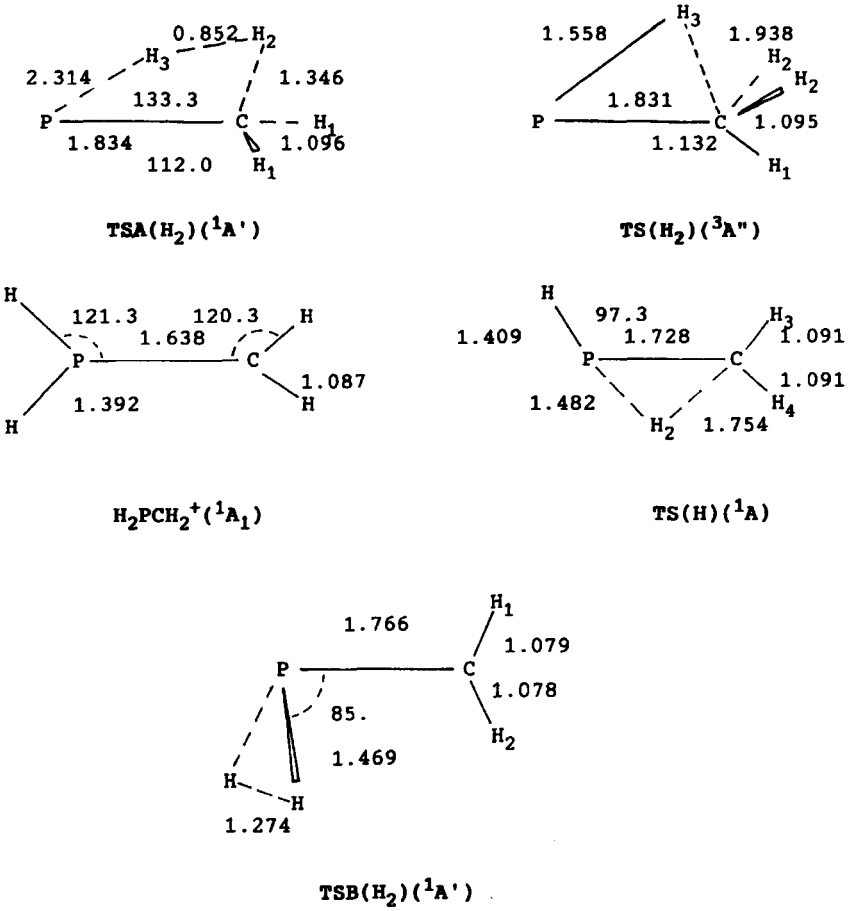

Figure 1. Geometries (Å and degrees) of the most relevant minima and saddle points of the potential surface corresponding to the $(PCH_4)^+$ system computed at the MP2(full)/6–31G* level, except for $PCH_4^+(^3A_2)$ and TSB$(H_2)(^1A')$ which were located at the MCSCF/6–31G* level. Geometrical parameters not shown in the figure are as follows. **HPCH$_3^+$**(^1A): $r(CH_3) = 1{\cdot}096$, $r(CH_2) = 1{\cdot}179$, $r(CH_1) = 1{\cdot}089$, $<PCH_3 = 115{\cdot}3$, $<PCH_2 = 102{\cdot}3$, $<HPCH_3 = 75{\cdot}2$, $<HPCH_2 = -37{\cdot}1$, $<HPCH_1 = 190{\cdot}7$. **HPCH$_3^+$**$(^3A'')$: $r(PH) = 1{\cdot}406$, $r(CH_1) = 1{\cdot}094$, $r(CH) = 1{\cdot}093$, $<HPCH = 180$, $<HPCH_1 = 60{\cdot}6$. **TS(H_2)**$(^3A'')$: $r(CH_1) = 1{\cdot}092$, $<PCH_2H_1 = 105{\cdot}8$, $H_3H_2C = 56{\cdot}0$. **TSA(H_2)**$(^1A')$: $r(CH_1) = 1{\cdot}096$, $<CH_2H_3 = 65{\cdot}2$, $<PCH_2H_1 = 116{\cdot}4$. TS$(H)(^1A)$: $r(CH_2) = 1{\cdot}754$, $<HPCH_3 = 10.8$, $<PCH_3H_4 = 180{\cdot}7$, $<PCH_3 = 125{\cdot}8$, $<PCH_4 = 118{\cdot}1$, $<H_1PCH_2 = 99{\cdot}1$. TSB$(H_2)(^1A')$ (MCSCF/6–31G**): $<H_1PCH_2 = 180$, $<HPCH_{2,1} = \pm 25{\cdot}9$

electrons for five orbitals. However, the G1 and G2 computations were made using the MP2(full)/6–31G* geometry, for coherence with of the rest of the species. The main difference between the two geometries is that the latter has a PHC bond angle of 107° rather than 180°, owing to the inability of the Møller–Plesset method to deal correctly with orbital near-degeneracy effects. Variation of the PHC angle, however, does not produce a significant change in the electronic energy energy, but it is important for the kind of dynamic calculation we pursue because of its effect on the rotational constant. The lowest three vibrational frequencies used in the dynamic computations were taken from the MCSCF/6–31G** computation. Basis set superposition effects[26] are not important because of the relatively large basis sets employed in the G1 and G2 methods; besides, the P—H bond is so strong that the mere definition of superposition error is unclear.

The other important minimum on the triplet PES is $HPCH_3^+(^3A'')$, which has a single P—C bond and lies 46·6 kcal/mol^{-1} (1 kcal = 4·184 kJ) below the ground state reactants (see Table 1). The collision complex $PCH_4^+(^3A_2)$ may isomerize into $HPCH_3^+(^3A'')$ via the transition state $TS(H)(^3A'')$, which is a saddle point on the PES of the $^3A''$ electronic state.

We studied two minima on the PES corresponding to the lowest singlet electronic state: $HPCH_3^+(^1A)$ that has a single P—C bond, and $H_2PCH_2^+(^1A_1)$, of C_{2v} symmetry, that has a double P—C bond. Both are connected by the transition state $TS(H)(^1A)$. $HPCH_3^+(^1A)$ is 23·9 kcal mol^{-1} lower than the corresponding triplet species $HPCH_3^+(^3A'')$; $H_2PCH_2^+(^1A_1)$ is the most stable species of the $(PCH_4)^+$ system.

$PCH_4^+(^3A_2)$ can be considered as the collision complex, it can dissociate directly into $PCH_2^+(^3A_2)$ through $TS(H_2)(^3A'')$, dissociate back into the reactants or isomerize into $HPCH_3^+(^3A'')$ through $TS(H)(^3A'')$; in the last process an intersystem crossing process (ISC) may take place, giving $HPCH_3^+(^1A)$. $HPCH_3^+(^3A'')$ may also produce $PCH_2^+(^3A_2)$ through $TS(H_2)(^3A'')$, or isomerize back into $PCH_4^+(^3A_2)$. The saddle points $TS(H_2)(^3A'')$ and $TS(H)(^3A'')$ lie just −5·2 and −8·6 kcal mol^{-1}, respectively, below the reactants (see Table 1).

According to our computations $HPCH_3^+(^1A)$ will not dissociate directly into $PCH_2^+(^1A_1)$, because the corresponding saddle point $TSA(H_2)(^1A')$ appears to be higher in energy than the reactants and $TS(H)(^1A)$ [i.e. the transition state for isomerization into the most stable species $H_2PCH_2^+(^1A_1)$] is much lower in energy. The latter species may produce $PCH_2^+(^1A_1)$ through the other transition state for hydrogen elimination on the singlet PES, $TSB(H_2)(^1A')$, that lies −40·2 kcal mol^{-1} below the reactants. Given that $TS(H)(^1A)$ and $TSB(H_2)(^1A')$ are so low in energy, the process $HPCH_3^+(^1A) \rightarrow PCH_2^+(^1A_1) + H_2$ is very fast, as we have checked by dynamic computations. In other words, intersystem crossing should end up, according to our results, in a quick dissociation into to the products in their singlet state.

It must be noted again that several transition states appear to be close in energy to the reactants. This may raise doubts about the reliability of our computations. It has been suggested that the transition states should be located at the QCISD/6–311G** level as the best one-determinant based method, the HF and MP2 levels may often be insufficient if the standard degree of accuracy of the G1 and G2 methods is sought.[27] For this reason, we relocated the saddle points $TS(H_2)(^3A'')$ $TS(H)(^3A'')$ and $TS(H_2)(^1A')$ at other levels of computation, namely MCSCF/6–31G, MP2(full)/6–31G**, MP2(full)/6–311G** and QCISD/6–311G**, but it turned out that the relatively small variation of the geometry does not produce a change in the electronic energy greater than the expected accuracy of G1 and G2 computations.

Table 1. G1 and G2 electronic energies (in hartree, without zero-point vibrational energies (ZPVE)], ZPVE (in kcal mol^{-1}) and relative energies (in kcal mol^{-1}) with respect to ground-state $P^+ + CH_4$[a]

Species	G1	G2	ZPVE	ΔG1	ΔG2
$P^+(^3P) + CH_4(^1A_1)$	−380·88744	−380·88994	29·1	0·0	0·0
$PH^+(^2\Pi) + CH_3(^2A_1)$	−380·83490	−380·83811	22·8	22·6	26·2
$PCH_2^+(^3A'') + H_2(^1\Sigma_g^+)$	−380·88938	−380·89188	21·7	−8·7	−8·7
$PCH_2^+(^1A_1) + H_2(^1\Sigma_g^+)$	−380·94435	−380·89188	20·6	−44·2	−43·9
$PCH_4^+(^3A_2)$	−380·93431	−380·93548	28·9	−29·6	−28·8
$HPCH_3^+(^3A'')$	−380·95984	−380·96309	28·4	−46·1	−46·6
$HPCH_3^+(^1A)$	−380·99755	−381·00033	27·9	−70·3	−70·4
$H_2PCH_2^+(^1A_1)$	−381·01841	−381·02077	27·6	−83·7	−83·6
$TS(H_2)(^3A'')$	−380·88816	−380·89060	24·3	−5·3	−5·2
$TS(H)(^3A'')$	−380·89538	−380·89811	25·6	−8·5	−8·6
$TSA(H_2)(^1A')$	−380·87462	−380·87689	25·8	4·7	4·9
$TS(H)(^1A)$	−380·97695	−380·97901	26·6	−58·4	−58·4
$TSB(H_2)(^1A')$	−380·94530	−380·94716	24·8	−40·6	−40·2

[a] MP2(full)/6–31G* geometries were used in all cases.

Schemes 1 and 2 illustrate the reaction paths we have proposed.

Note that the triplet–singlet conversion (ISC) may take place either during the $PCH_4^+(^3A_2) \rightleftharpoons HPCH_3^+(^3A'')$ isomerization process or after $HPCH_3^+(^3A'')$ is formed. While the lowest singlet state is 35 kcal mol^{-1} higher in energy than $PCH_4^+(^3A_2)$ at the MP4/6–311G** level, it lies clearly below TS(H)($^3A''$), i.e. the PES corresponding to the lowest singlet and triplet electronic states cross at some point along the reaction coordinate. This situation may trigger a non-adiabatic process (ISC) resulting in $HPCH_3^+(^1A)$, through spin–orbit coupling between the singlet and triplet electronic states. The $HPCH_3^+(^3A'') \rightleftharpoons HPCH_3^+(^1A)$ transition may be prompted by the wide energy gap between the two species (23·8 kcal mol^{-1}), and by the fact that, according to our dynamic computations, the triplet state would be relatively long-lived, its average lifetime at 300 K being 1300 ps.

Unfortunately, a reliable computation of the rate coefficients for ISC in a complex molecule is a very difficult task,[15] and is at present beyond our capabilities. However, we shall try to show that by combining our theoretical results with the experimental results, one may draw some conclusions about the role of intersystem crossing which, although only tentative, still help in understanding the dynamics of this reaction.

As we have stated above, whenever $HPCH_3^+(^1A)$ is formed, fast isomerization into $H_2PCH_2^+(^1A_1)$ will follow; this species will immediately dissociate into the products in their singlet state. This implies that the reaction dynamics are controlled by the collision step (k_c), the dissociation into the reactants (k_d) and products (k_{TS1}), the $PCH_4^+(^3A_2) \rightleftharpoons HPCH_3^+(^3A'')$ isomerization (k_{TS2}, k_{-TS2}), dissociation of $HPCH_3^+(^3A'')$ into products (k_2) and the intersystem crossing [$k_{ISC(1)}$ and $k_{ISC(2)}$].

The collision step was studied by means of an approximate classical trajectory method that incorporates contributions from ion–induced dipole and ion–quadrupole interactions that account for the long-range potential, and also 'chemical' interactions through a Morse potential obtained by fitting an *ab initio* energy profile obtained at the PMP2/6–311G(2df, p) level (spin projected second-order Møller–Plesset[23]). It must be noted that this approach gives a capture rate for 300 K higher than the value reported by Smith *et al.*[4] ($k_c = 1{\cdot}15$ cm^3 s^{-1} molecule^{-1}), due almost entirely to the lack of ion–quadrupole interactions in the latter computation.

An important question should be raised when one includes the capture step in a dynamic scheme such as that shown in Scheme 1, namely whether k_c should be corrected for the fraction of attractive PES that is nearly degenerate at large separations of the reactants.[10,12] CIS/6–311G** computations[28] (a configuration interaction method including single substitutions of the reference determinant) on the geometry of $PCH_4^+(^3A_2)$ indicate that the two lowest excited triplet states lie 28·5 kcal mol^{-1} above the reactants, even though they have virtually the same energy as the ground state for $r(PH) > 5$ Å. One is tempted to correct k with a factor $f = 1/3$, but then the upper limit for the total rate constant would be $k_{bim} = k_c/3$. Given that k_c is computed fairly accurately,[12] and our value for 300 K is 1·29 cm^3 s^{-1} molecule^{-1}, the resulting upper limit is inconsistent with the experimental results

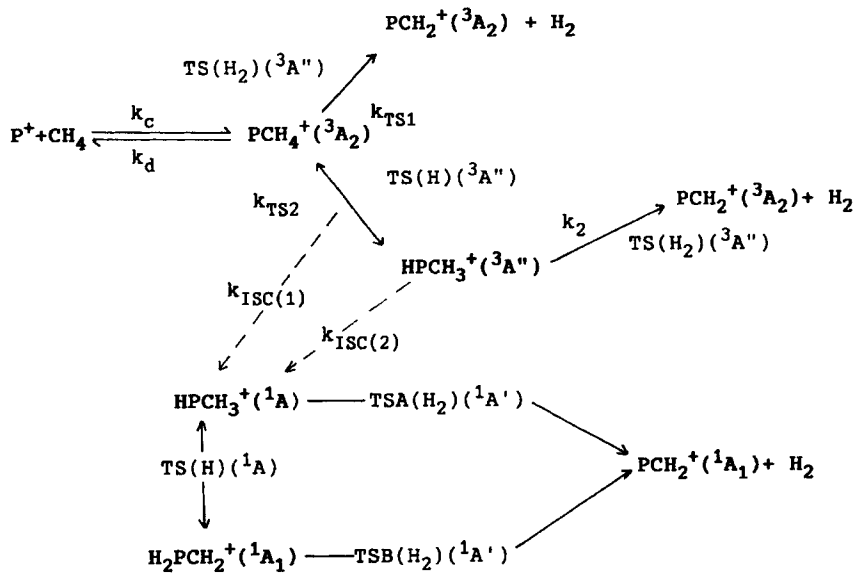

Scheme 1. Possible reaction paths for the reaction of P^+ with methane

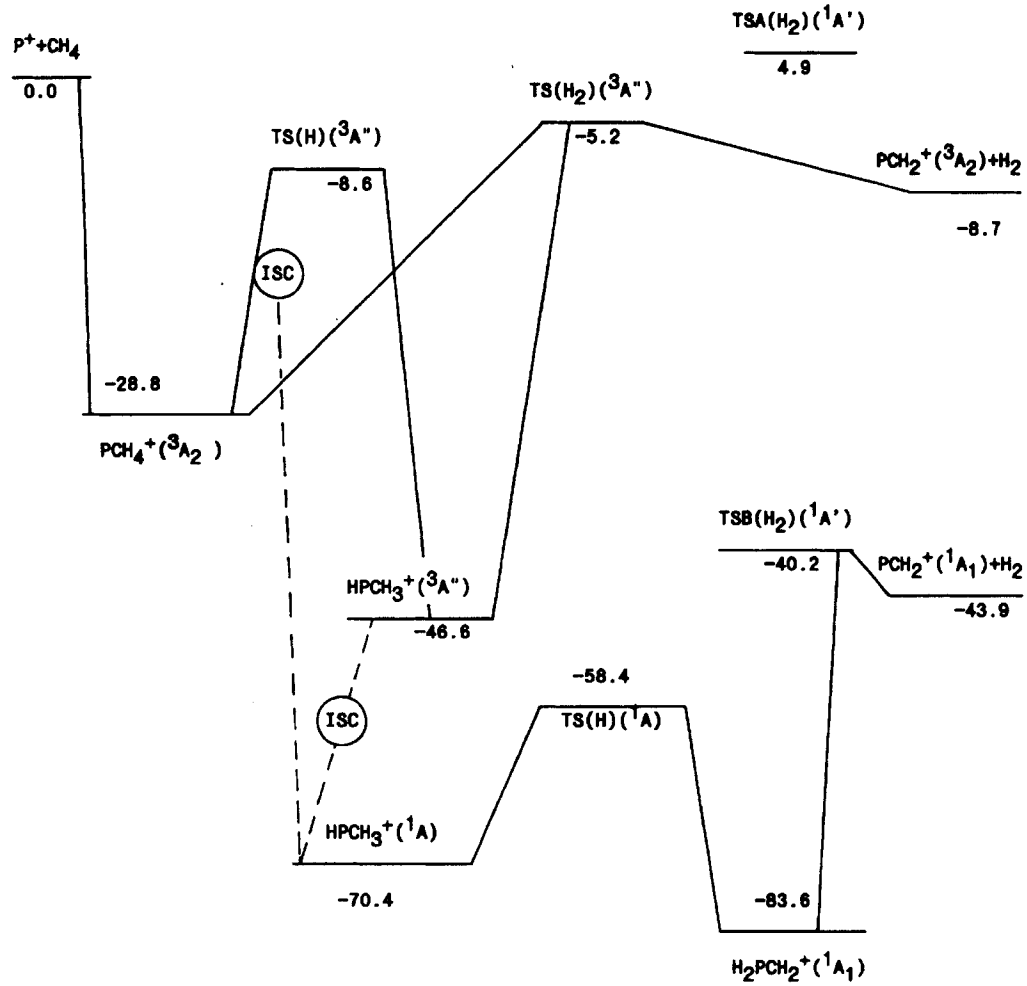

Scheme 2. Energy diagram for the reaction of P^+ with methane. Energies in kcal mol^{-1}

[$k_{bim} = 9{\cdot}4 \times 10^{-10}$ (Ref. 3) or $9{\cdot}6 \times 10^{-10}$ $cm^3 s^{-1}$ $molecule^{-1}$ (Ref. 4)]. We may conclude that the system is probably complex enough that relaxation into the electronic ground state is fast, although we must also admit that we cannot be sure the relaxation is complete.

Computation of k_d presents several difficulties. First, there is no saddle point for this process; in order to determine the transition state we used variational transition-state theory in its canonical form;[15,29] this was done for each temperature that we selected in the present study. Another difficulty is the treatment of two internal degrees of freedom corresponding to the motion of the CH_4 group about the P—C axis; for low values of r(PH) the potential is still deep and these motions behave like vibrations, and when the P—H distance increases they behave more like rotations. In order to deal with the changing nature of these internal degrees of freedom, we employed a sinusoidally hindered rotor model, including also steric interactions through a hard sphere model, as proposed by Schmidt and Gilbert and co-workers (see Refs 15 and 16 for details), in a computation that explicitly conserves angular momentum. The variationally determined transition states lie very close to $r(PH) = 4{\cdot}8$ Å for all temperatures except the very low ones, where it moves up to $r(PH) = 5{\cdot}1$ Å. Another difficulty, which we did not confront in the present study, is the inclusion of quantum states corresponding to the two electronic excited states that become nearly degenerate to the ground state for high r(PH). It must be noted, however, that the location of the corresponding PES combined with the results of the variational determination of the transition states suggest

that inclusion of the quantum states coming from the excited electronic states would reduce the r(PH) distance of the transition state, but the k_d values should not increase significantly.

Table 2 presents some of the results of our computations. The third column contains the results obtained without taking into account ISC [$k_{ISC(1)} = 0$, $k_{ISC(2)} = 0$]. The value for 300 K is clearly lower than the experimental values. Given that (i) the computation of TS(H)($^3A''$) and TS(H_2)($^3A''$) can be considered accurate and (ii) the k_d values could be slightly lower than the exact values, we consider this difference between the computed and experimental results to be significant, clearly suggesting-that ISC may indeed play a role in this reaction.

This result was not unexpected, as we had already concluded that the most important reaction intermediate in the reaction of P^+ with water is $HPOH^+(^1A')$, which is produced from the collision complex via ISC.[8]

In order to gain more insight, we propose two simple models to deal with ISC in this case.

(a) We have defined a combined isomerization and ISC microscopic rate coefficient for $PCH_4^+(^3A_2)$ as $(1-P)k_{TS2}(E) + Pk_{ISC(1)}(E)$ with $k_{ISC(1)}(E) = \xi k_{TS2}(E)$, where ξ is constant and P represents the probability of ISC relative to the adiabatic isomerization process. An alternative way of writing the former expression is $(1+\alpha)k_{TS2}(E)$; for simplicity we consider α to be independent of E, it is just a parameter that we select for coincidence between the computed and experimental k_{bim}(300 K) values. In this model $k_{ISC(2)} = 0$, i.e. the rate constant for the ISC process $HPCH_3^+(^3A'') \rightarrow HPCH_3^+(^1A)$ is set to zero.

(b) We use the same model but this time we take $k_{ISC(2)} = 10^{12}\ s^{-1}$. We found that for $k_{ISC(2)} > 10^{12}\ s^{-1}$ and $\alpha = 0$, the computed rate constant reaches a limit $k_{bim}(300\ K) = 9{\cdot}1 \times 10^{-10}\ cm^3\ s^{-1}$ molecule^{-1}, still lower than the experimental result. Now we also vary α until we find agreement between the computed and experimental values of k_{bim} (300 K).

The computed values of k_{bim} are given in Table 2. Both models produce basically the same rate constants and very similar average lifetimes for $PCH_4^+(^3A_2)$, not only at 300 K (as it must be according to the definition of the models) but for the whole range of temperatures. k_{bim} increases only slightly with decrease in temperature, because of both the increase in the capture rate and the decrease in k_d(E), which is much faster than in the case of the other rate coefficients of $PCH_4^+(^3A_2)$; both effects are not unexpected.[12] The difference between the capture and total rates increases with increase in temperature; it is clear that for low temperatures the reaction dynamics are fully determined by the capture step.

It must be pointed out that the average lifetime of $PCH_4^+(^3A_2)$ ranges from 16 ps at 40 K to 5 ps at 1000 K, hardly depending on the model employed. However, the lifetime of $HPCH_3^+(^3A'')$ is extremely sensitive to the values of $k_{ISC(2)}$ and can range from 1300 ps for $k_{ISC(2)} = 0$ to just about 1 ps for $k_{ISC(2)} = 10^{12}\ s^{-1}$ (300 K); in other words, in the absence of the second ISC process, this species should be relatively long-lived, as we pointed out above.

Table 2. Computed rate coefficients for the complete reaction, k_{bim}, and the capture step, k_c, in units of $cm^3\ s^{-1}$s molecule^{-1}, for the two models employed (see text)[a]

		$k_{bim} \times 10^9$		
T/K	$k_c \times 10^9$	$k_{ISC(1,2)} = 0$	$k_{ISC(2)} = 0$	$k_{ISC(2)} = 10^{12}$
40	1·65	1·61	1·63	1·63
60	1·55	1·48	1·52	1·52
80	1·49	1·40	1·45	1·45
100	1·44	1·15	1·30	1·30
120	1·40	1·04	1·24	1·24
140	1·38	1·00	1·19	1·38
160	1·36	0·93	1·12	1·13
180	1·34	0·88	1·09	1·09
200	1·33	0·85	1·05	1·06
220	1·32	0·82	1·03	1·03
240	1·31	0·79	1·00	1·01
260	1·31	0·77	0·98	0·99
280	1·30	0·74	0·97	0·98
300	1·29	0·72	0·96	0·96
340	1·29	0·69	0·93	0·93
420	1·27	0·64	0·88	0·88
580	1·25	0·58	0·81	0·81
800	1·22	0·52	0·74	0·73
1000	1·19	0·49	0·68	0·67

[a]For the capture model we employed $\alpha = 2{\cdot}567 \times 10^{-24}\ cm^3$ and $Q_{xx} = Q_{yy} = Q_{zz} = -8{\cdot}41$ DD Å for CH_4. Details of the computations, such as vibrational frequencies, are available from the author on request.

CONCLUSIONS

We have carried out a theoretical study of the reaction of P^+ with methane, by means of an approach that combines an approximate classical trajectory method and RRKM theory. In order to apply it, we computed the most important minima and saddle points on the PES corresponding to the lowest, lying singlet and triplet electronic states at the G1 and G2 levels of theory.

The experimental value of the rate coefficient, that was obtained at 300 K, could not be explained without assuming that intersystem crossing takes place. This hypothesis is supported by our experience with the reaction of P^+ with water.

Our computations also suggest that whenever the singlet state is generated it will very quickly dissociate into the products.

We have presented computed values of k_{bim} for a wide range of temperatures, ranging from 40 to 1000 K. There is only a moderate increase in reaction rate with

decrease in temperature, which is prompted by the increase in the capture rate and by other dynamic effects.

ACKNOWLEDGEMENTS

The author acknowledges financial support from the University of Valladolid (Programa de Ayuda a Jóvenes Investigadores).

REFERENCES

1. L. R. Thorne, V. G. Anicich, S. S. Prasad and W. T. Huntress, Jr, *Astrophys. J.* **280**, 139 (1984).
2. N. G. Adams, B. J. McIntosh and D. Smith, *Astron. Astrophys.* **232**, 443 (1990).
3. L. R. Thorn, V. G. Anicich and W. T. Huntress, *Chem. Phys. Lett.* **98**, 162 (1983).
4. D. Smith, B. J. McIntosh and N. G. Adams, *J. Chem. Phys.* **90**, 6213 (1989).
5. A. Largo, J. R. Flores, C. Barrientos and J. M. Ugalde, *J. Phys. Chem.* **95**, 6553 (1991).
6. S. Wilson, *Chem. Rev.* **80**, 263 (1980).
7. J. A. Pople and R. K. Nesbet, *J. Chem. Phys.* **22**, 571 (1954); R. Seeger and J. A. Pople, *J. Chem. Phys.* **66**, 3045 (1987).
8. J. R. Flores and P. Redondo, *Chem. Phys. Lett.* **230**, 358 (1994).
9. J. R. Flores and P. Redondo, *Chem. Phys. Lett.* **240**, 193 (1995).
10. C. E. Dateo and D. C. Clary, *J. Chem. Phys.* **90**, 7216 (1989).
11. L. F. Phillips, *J. Comput. Chem.* **11**, 88 (1990).
12. L. F. Phillips, *Prog. Energy Combust. Sci.* **18**, 75 (1992).
13. L. F. Phillips, *J. Phys. Chem.* **94**, 5265 (1990).
14. R. G. Gilbert, *QCPE Bull.* **3**, 64 (1983).
15. R. G. Gilbet and S. C. Smith, *Theory of Unimolecular and Recombination Reactions*. Blackwell, Oxford (1990).
16. S. C. Smith, P. P. Wilson, P. Sudkeaw, R. G. A. R. McLagan, M. J. McEwan, V. G. Anicich and W. T. Huntress, *J. Chem. Phys.* **98**, 1994 (1993).
17. L. A. Curtiss, C. Jones, G. W. Trucks, K. Raghavachari and J. A. Pople, *J. Chem. Phys.* **93**, 2537 (1990).
18. L. A. Curtiss, K. Raghavachari, G. W. Trucks and J. A. Pople, *J. Chem. Phys.* **94**, 7221 (1991).
19. Krishnan, R. and J. A. Pople, *Int. J. Quantum. Chem.* **14**, 91 (1978).
20. M. M. Francl, W. J. Petro, W. J. Hehre, J. S. Binkley, M. S. Gordon, D. J. DeFrees, and J. A. Pople, *J. Chem. Phys.* **77**, 3654 (1982).
21. B. O. Ross, *Int. J. Quantum. Chem. Symp.* **14**, 175 (1980).
22. J. A. Pople, M. Head-Gordon, D. J. Fox, K. Raghavachari and L. A. Curtiss, *J. Chem. Phys.* **90**, 5622 (1989).
23. H. B. Schlegel, *J. Chem. Phys.* **84**, 4530 (1986).
24. M. J. Frisch, M. Head-Gordon, G. W. Trucks, J. B. Foresman, H. J. Schlegel, K. Raghavachari, M. A. Robb, J. S. Binkley, C. Gonzalez, D. J. DeFrees, D. J. Fox, R. A. Whiteside, R. Seeger, C. F. Melius, J. Baker, R. L. Martin, L. R. Kahn, J. J. P. Stewart, S. Topiol and J. A. Pople, *Gaussian 90*. Gaussian, Pittsburgh, PA (1990).
25. M. W. Schmidt, K. K. Baldridge, J. A. Boutz. J. M. Jensen, S. Koseki, M. S. Gordon, K. A. Nguyen, T. L. Windus and S. T. Elbert, *QCPE Bull.* **10**, 57 (1990).
26. S. F. Boys and F. Bernardi, *Mol. Phys.* **19**, 553 (1970).
27. J. L. Durant and C. M. Rohlfing, *J. Chem. Phys.* **98**, 8031 (1993).
28. J. B. Foresman, M. Head-Gordon, J. A. Pople and M. J. Frisch, *J. Phys. Chem.* **96**, 135 (1992).
29. B. C. Garret and D. G. Truhlar, *J. Phys. Chem.* **83**, 1052 (1979).